Supporting information for

A Hydrodynamically Optimized Nano–Electrospray Ionization Source and Vacuum Interface

Matthias Pauly[1], Mario Sroka[2], Julius Reiss[2], Gordon Rinke[1], Alyazan Albarghash[1], Ralf Vogelgesang[1], Hannes Hahne[3], Bernhard Kuster[3], Jörn Sesterhenn[2], Klaus Kern[1,4], Stephan Rauschenbach[1*]*

[1]Max-Planck-Institute for Solid State Research, Heisenbergstr. 1, DE–70569 Stuttgart, Germany
[2]Technical University Berlin, Str. des 17. Juni 135, DE–10623 Berlin, Germany
[3]Chair of Proteomics and Bioanalytics, Technische Universität München, Emil-Erlenmeyer-Forum 5, DE–85354 Freising-Weihenstephan, Germany
[4]Institut de Physique de la Matière Condensée, Ecole Polytechnique Fédérale de Lausanne, CH–1015 Lausanne, Switzerland
[*]Corresponding author email: matthias.pauly@ics-cnrs.unistra.fr, s.rauschenbach@fkf.mpg.de

Summary

In the main article, we present a nano–electrospray ionization vacuum interface reaching 100% transmission using a capillary with an inlet, optimized to exploit the hydrodynamic drag of the background gas for collimation and the reduction of space charge repulsion. In this Supporting Information, a detailed view of the ion source is given in Section I. The precise experimental procedure for measuring the ionic current on the capillary and in vacuum is presented in Section II. Details about the computational fluid dynamics (CFD) calculations are given in Section III. The calculated characteristics of the gas flow through the interface have been used to simulate the ion trajectories using SIMION, which is presented in Section IV. In order to prove the high quality of the transmitted ion beam, CytC protein ions have been deposited in ultrahigh vacuum following a procedure detailed in Section V. Mass spectra obtained on a commercial mass spectrometer on which the optimized ion source has been implemented are shown in Section VI. The temperature dependence of the transmission current through the funnel interface is shown in section VII. Finally in sections VIII we comment on the sampling efficiency and show in section IX that our data is reproducible.

S-I/ Sketch of the Vacuum Interface

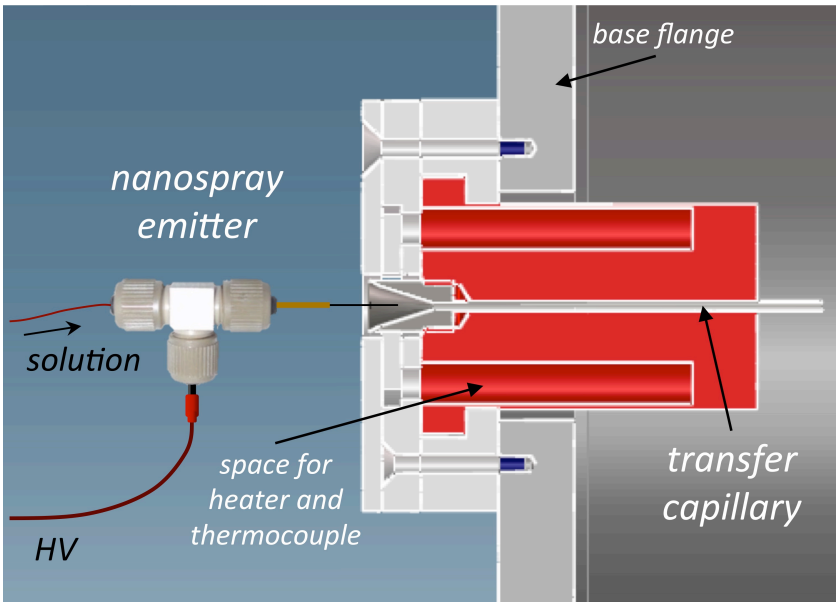

Figure S-1: Cross section of the vacuum interface. The length of the capillary including the funnel is 7cm.

The atmospheric interface consists of the capillary itself, a copper cylinder, and PTFE insulator discs. It is mounted on an ISO-K 100 base flange with a center symmetric hole of 36 mm inner diameter. Two PTFE discs, fixed with six screws directly to the base flange, hold the copper block in place and isolate it electrically. These discs serve as vacuum gaskets also. Four holes of 6 mm diameter run 5 cm deep into the copper cylinder from the atmospheric pressure side. Inside them the heater elements and the thermocouple are fitted. In the center a hole of 2 mm in diameter runs through the whole length of the copper cylinder. On the high pressure side of this hole a M8 thread is cut, used to mount the capillaries.

The capillary itself consists of a thin stainless steel tube (inner diam.: 1 mm, outer diam.: approx. 1.5 mm), which is soldered into a stainless steel cylinder of 1 cm length and 8 mm diameter. An M8 thread is cut in the steel cylinder for mounting it onto the copper block. On the other side it opens to air in flat or funnel geometry (Figure S-1 shows the funnel version). The capillary makes good thermal contact to the heated copper block .

The electric wiring for the heater cartridges, for the thermometer (Pt100) and for the high voltage/current measurement is guided in channels inside the PTFE discs and appears at the atmosphere side of the assembly, where plugs are fitted to the cables. The whole assembly is finally

covered with a third PTFE disc such that only the actual interface is accessible from the outside, thus minimizing the risks of accidentally touching the high voltage electrode during operation.

S-II/ Transmission Characteristics: Experimental Details

The transmission characteristics of the ion source have been investigated by measuring the current on the ion transfer capillary and on a metal plate hold in vacuum 1 cm downstream of the capillary exit, the total emitted current being the sum of the current transmitted in vacuum and the current measured on the ion transfer capillary. Both the capillary and the metal plate were grounded, while a high voltage ($V_{emitter}$ = 0-5 kV) was applied to the emitter. The emitted current and the transmitted current may vary for different emitters, although the general behavior stays constant. The highest current transmitted in vacuum we have recorded with the funnel-shaped capillary (diameter: 1 mm) was 40 nA (see Figure S-2). The usual procedure for measuring the current was as follows:

The *zero* position for the emitter, which is mounted on a moveable xyz stage, is first determined by placing the emitter exit on the capillary axis and at its entrance. The emitter is then positioned at the desired position and the solution is infused to the emitter with a syringe pump via a PEEK union in which a metallic electrode is inserted to apply the high voltage. The voltage is slowly increased until a stable electrospray forms (usually at 1-1.5 kV). For the measurement of the current as function of the emitter voltage (Figure 2a–f), the position of the emitter was maintained constant through the experiment (r = 0 mm and z = −5 mm for the flat capillary and z = −10 mm for the funnel capillary). For each RhoB solution (concentration10^{-5}–10^{-2} M, the lowest concentrations have been measured first), the voltage was varied from 1 to 5 kV in 0.25 kV increments and then from 5 to 1 kV. No hysteresis has been observed when sweeping the voltage up or down. The data presented in the Figure 2a-f are the average of these two values.

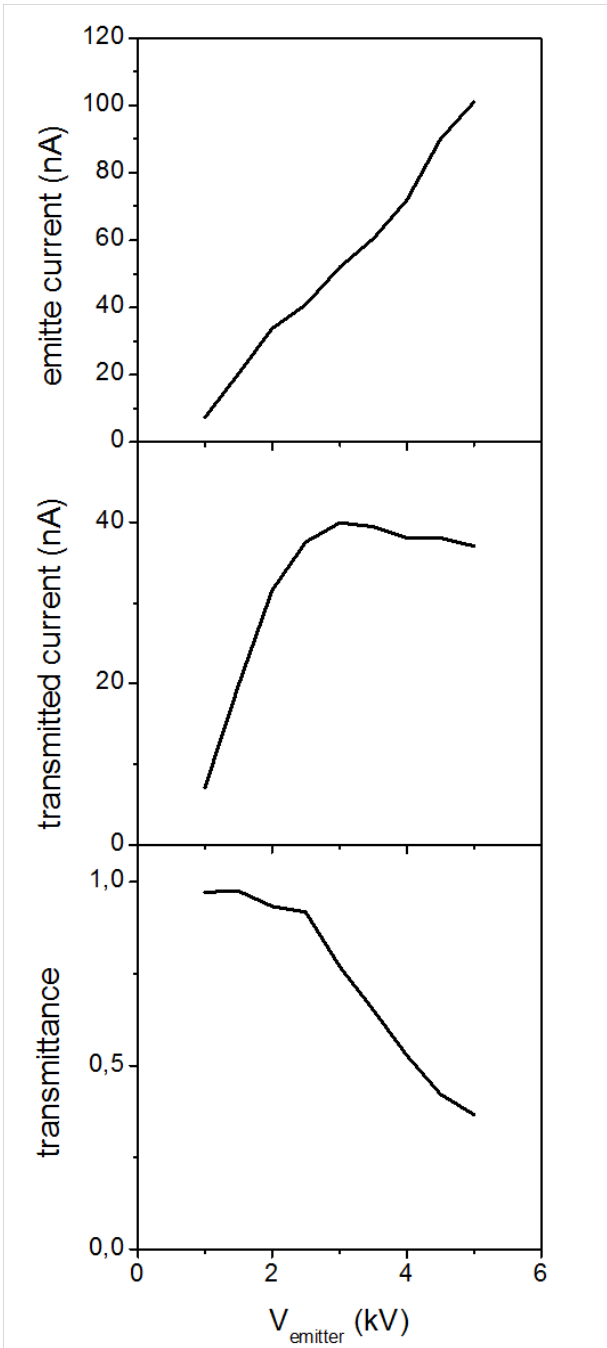

Figure S-2: emission and transmission characteristics showing high transmitted current in vacuum for a 10^{-4} M solution as function of the voltage applied to the emitter. Depending on the emitter characteristics, the current transmitted to vacuum may vary. The data presented here are representative of the highest current recorded in vacuum for the funnel shaped 1 mm diameter capillary.

For the measurement of the current as function of the emitter position (Figure 3), the voltage has been held constant ($V_{emitter}$ = 2.5 kV) and the currents have been measured for the 10^{-4}M RhoB solution. A first set of measurements has been made by varying the radial position *r* for 4 different azimuthal positions (*z* = −1, −3, −6 and −9 mm for the flat capillary and *z* = −2, −5, −8 and −11 mm for

the funnel capillary). A second measurement has been performed by varying the azimuthal position (between $z = -10$ and $z = -1$ mm for the flat capillary and $z = -20$ and $z = -2$ mm for the funnel capillary) while keeping the emitter on axis ($r = 0$ mm). These measured data are given in Figure S-3. These data have been extrapolated to a matrix in order to construct the color plot presented in Figure 3.

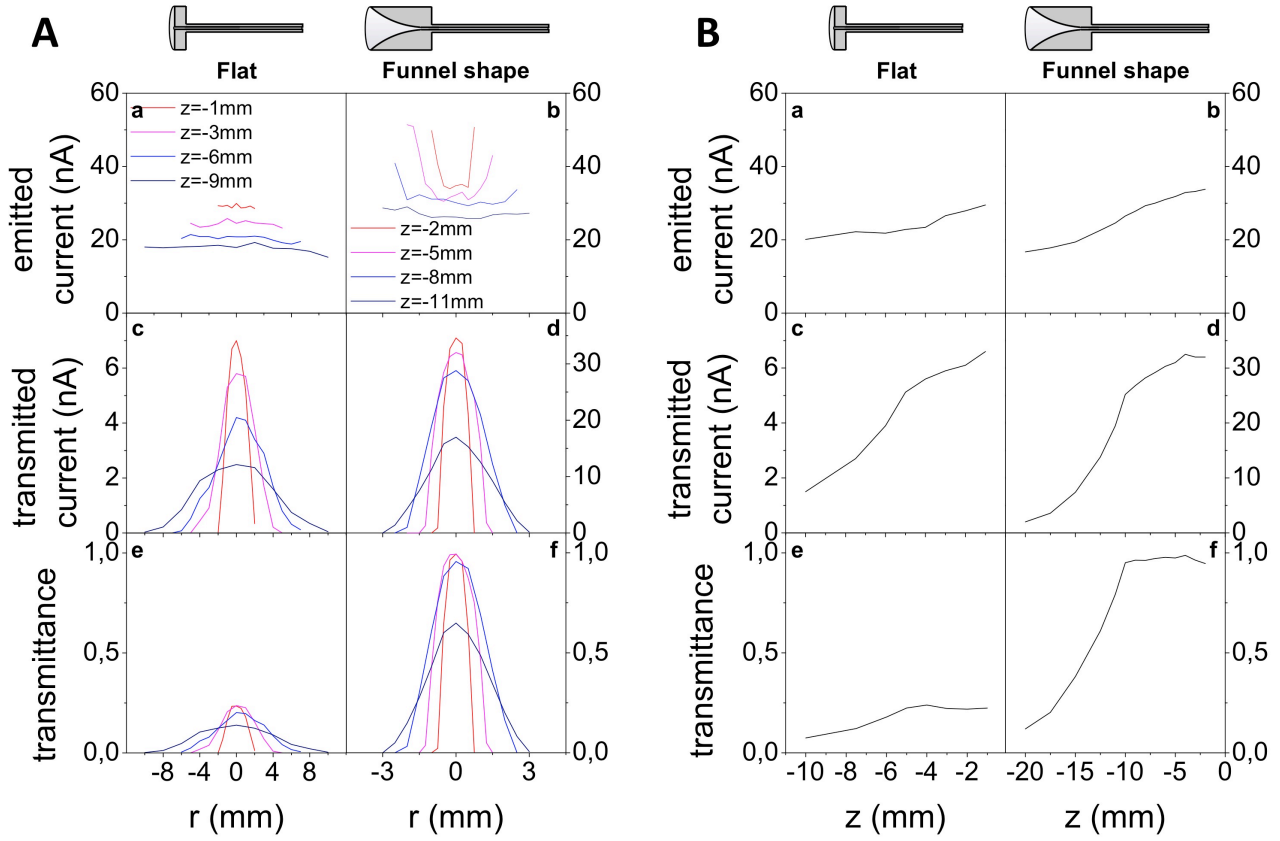

Figure S-3: a-f) emission and transmission characteristics for the flat (a, c, e) and funnel-shaped (b, d, f) capillaries for a 10^{-4}M RhoB solutions with a constant voltage of 2.5kV applied to the emitter as function of the radial position r (**pannel A**) and as function of the azimuthal positions z for r = 0 mm (**pannel B**). a, b) total current emitted from the emitter; c, d) current transmitted in vacuum; e, f) transmittance, defined as the ratio between the current transmitted in vacuum and the total emitted current.

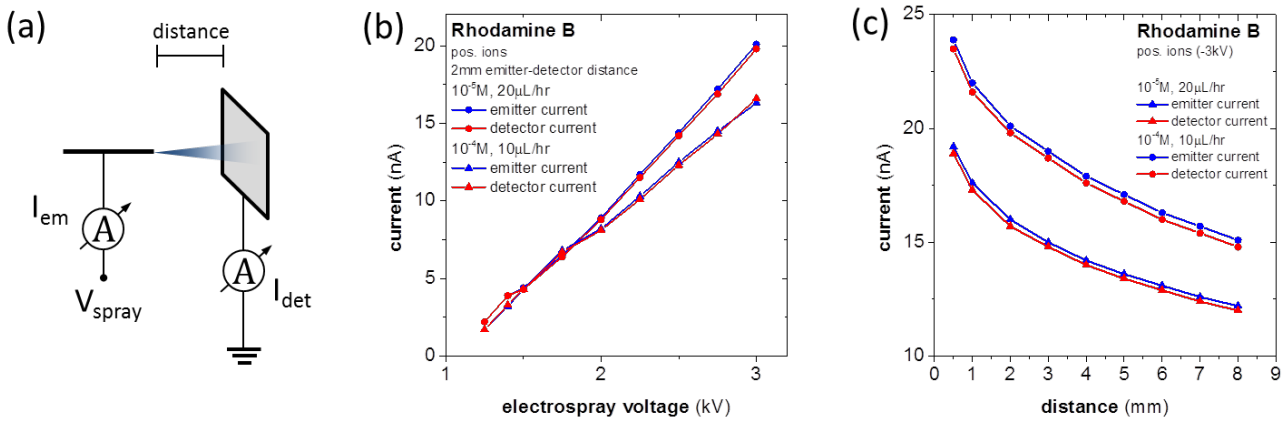

Figure S-4: a) Layout of the reference experiement. b) Absolute value of emitted and collected current as function of the electrospray voltage and c) as a function of the distance.

To confirm the validity of the relation $I_{emitted} = I_{capillary} + I_{transmitted}$, we tested a simplified setup as shown in Fig. S-4a, where emitted current and a detector current are measured only. The fact that for varying the electrospray voltage as well as the distance both currents are always the same indicates that no additional loss current exits.

S-III/ Computational Gas Dynamic Calculations

General

The two-dimensional Navier-Stokes equations are simulated, assuming a Newtonian friction. The friction is modeled by the Sutherland law:

$$\mu = \mu_0 \left(\frac{T}{T_0}\right)^{3/2} \left(\frac{T_0 + 110.4}{T + 110.4}\right)$$

where the standard parameters for air have been used $\mu_0 = 8.1720 \times 10^{-5}$, $T_0 = 300$ K. The heat conductivity was connected by constant Prandtl Number of $Pr = 0.71$.

The ***main source of error*** is assumed to be the two dimensionality of the flow calculation. Some improvement can be expected by a rotational symmetric configuration, thus working in spherical coordinates. A fully reliable simulation is expected only for a truly three dimensional flow. However turbulence is expected only beyond the inlet of the capillary. A study of a complete interface should therefore either model or resolve turbulences in three dimensions. Other errors, spatial and temporal errors are assumed to be less important, thus no detailed convergence study was done.

Method

The simulation was done in a characteristic rewriting of Navier-Stokes equations described by Sesterhenn et al.[1] This code is original designed for Direct Numerical Simulation (DNS) and aero-acoustic simulations. Here instead of high order, a 1st order upwind derivative to have quick convergence and a fourth order Runge Kutta time stepping is used. For given inflow and outflow conditions the flow is simulated in time, until a steady state is reached. A steady state is considered if the change in kinetic energy is small.

Simulation Grid

Boundary fitted grids are used. For the straight capillary a global Cartesian, but not rectangular grid was made. For the funnel-shaped nozzle a curvilinear grid is created, which is made nearly orthogonal by a grid smother.

The resolution of the capillary is $N_x = 200$, $N_y = 200$, where the capillary starts at 100 and has 16 grid points diameter.

The resolution of the funnel-shaped nozzle is $N_x = 164$, $N_y = 70$.

Boundary conditions

The boundary conditions are a non slip wall at the shape of the nozzle and a symmetry condition at the symmetry axis. The inflow and outflow were done by a sponge layer of the first grid points, i.e. artificial force terms in the equations which act on pressure, inflow velocity and entropy at the inlet and the pressure at the outlet.

S-IV/ Ion Trajectory Simulations

A) Interactions of an ion and a moving gas

An ion of mass *M* moving in a background gas of particles of mass *m*, pressure *p* and temperature *T* will undergo frequent collisions. Since this process is random and the conditions of each collision cannot be known it can be characterized statistically for instance by giving the mean free path length:

$$\lambda = \left(n\pi\sigma \sqrt{\frac{M}{m}} \right)^{-1}$$

Here $n = pNA/RT$ is the density of the gas and $\sigma = \pi(r_1+r_2)^2$ the hard sphere cross section of the collision. By this relation the mean free path of a heavy ion like Rhodamine B (M = 443 u) at ambient pressure (1 bar) at room temperature calculates to 28 nm. For heavier ions it would be even smaller. In each collision energy is transferred between the collision partners, thermalizing the gas. The maximal collision energy can be calculated from momentum and energy conservation as

$$E = \frac{\mu}{2}(v_1 - v_2)^2$$

With the reduced mass $\mu = m_1m_2/(m_1+m_2)$.

Similarly characteristic, the average velocity is be given by

$$\bar{v} = \sqrt{\frac{8kT}{\pi m}}$$

and calculates to 470 m/s for nitrogen and 118 m/s for RhoB.

If we consider a moving background gas in which heavy ions are dispersed, we can ask on which length scale they are following the motion of the background gas. To approximate that, we sum up the energy transfer until a given difference in kinetic energy is met. For a number of k collision this can be written as:

$$E(k) = E_0\left(1 - \frac{2\mu}{m_{ion}}\right)^k$$

Placing for instance resting RhoB ions in a gas moving at a velocity of 200 m/s, the maximum we found in the computational fluid dynamics simulations, we can calculate that such ions would be thermalized after 17 collisions, which corresponds to a distance traveled of less than 500 nm. With the gradient of gas velocity in our system being less than 100 m/s per millimeter, it is clear that without other external forces Rhodamine ions can be assumed to follow the path of the background gas almost exactly.

B) Effect of ion diffusion

One possible ion loss mechanism within the capillary is diffusion.[2] To evaluate its influence on the ion transport in the transfer capillary, we first consider the diffusion coefficient of a diluted concentation of heavy ions (X) in air

$$D = \frac{4}{3}\frac{T^{\frac{3}{2}}}{p(d_{air} + d_X)^2}\sqrt{\frac{{k_B}^3}{\pi^3}}\sqrt{\frac{1}{2M_{air}} + \frac{1}{2M_X}}$$

for a gas temperature of T = 500 K at a pressure p = 800 mbar, with M_{air} =29 u, M_X = 443 u and d_X = 9.1 Å, d_{air} = 3.7 Å for the masses and particle diameters of RhoB and air respectively. We find a diffusion constant of 0.035 cm^2/s. The gas passes the 60 mm long capillary at a velocity of 200 m/s which relates to a residence the of 0.3 ms which we use to estimate the diffusion length of a rhodamine ions moving with the gas

$$L = \sqrt{D\ t_{res}} \approx 32\ \mu m$$

This value is more than an order of magnitude below the capillary radius (0.5 mm) and the space-charge-driven diffusion length, calculated as 0.6 mm for a 100 nA current (see manuscript). It can thus be concluded that losses due to diffusion of ions toward the capillary wall plays a negligible role in our case.

A more sophisticated consideration was used by Sunner et al.[2] calculating a critical charge density for which the losses due to space charge expansion become larger than those of diffusion.

$$\rho_{sc} = kT\frac{\varepsilon_0}{ze}\left(\frac{2.4}{r}\right)^2$$

For our geometry and a gas velocity of 200 m/s we find a critical current of approximately 1 nA, which is well below the currents we consider in this paper and therefore we can neglect diffusion losses when describing the behaviour of the funnel capilalry source.

C) Ion motion in a gas flow and an eletromagnetic field

The ion motion in the interface were simulated using SIMION[3] with the SDS package[4] to include the influence of a neutral background gas in motion. The potential array has been constructed to match exactly the geometry of the capillaries used in the experiments. The fluid flow calculations were reparameterized to fit the 65×445 cell potential array with cylindrical symmetry (1 graphical unit = 0.1 mm, see figure S-5). These arrays have been refined and for the ion trajectory simulations 2.5 kV at the emitter electrode and 0 V to the capillary electrode are applied.

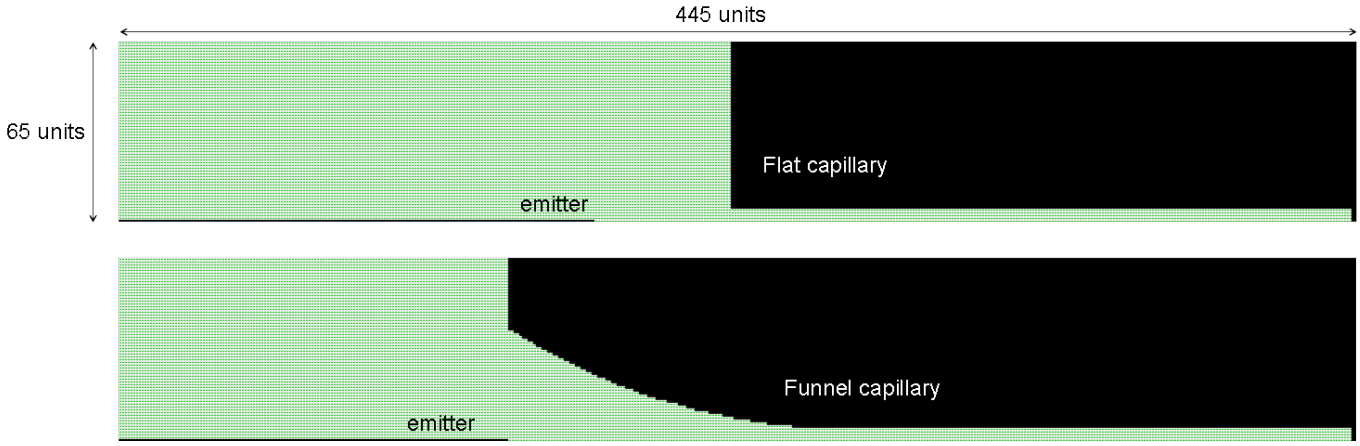

Figure S-5: potential arrays used for the flat and the funnel capillary for the simulations with SIMION.

The SDS (Statistical Diffusion Simulation) is a user program for SIMION that simulates motions of charged particles under finite pressure conditions in electrostatic fields. Ion motions are simulated by a combined viscous ion mobility and random ion jumping approach. The gas pressure as well as the velocity in azimuthal and radial directions have been reparameterized from the computational fluid dynamics calculations for each point of the grid (Figure 4a-c). Ions with a mass and charge similar to RhoB ions (m = 443 and z = +1) have been used for the simulation. Air has been used as the background gas (m = 28.945, collision diameter = 3.66 Å) and the temperature has been set constant to 300 K. The ion's reduced mobility is estimated by SIMION from the ion mass to $K_0 = 9.2\times10^{-5}$ $m^2V^{-1}s^{-1}$ and the collision diameter to 9.17 Å.

Ions are started from a straight line 2.5 mm beyond the capillary. The trajectories plotted on figure 4a are the average over 10 trajectories spread with a 0.4 mm step between r = 0 mm and r = 1.6 mm (Figure S-6). Since space charge forces are not considered all ions are transmitted in these simulations.

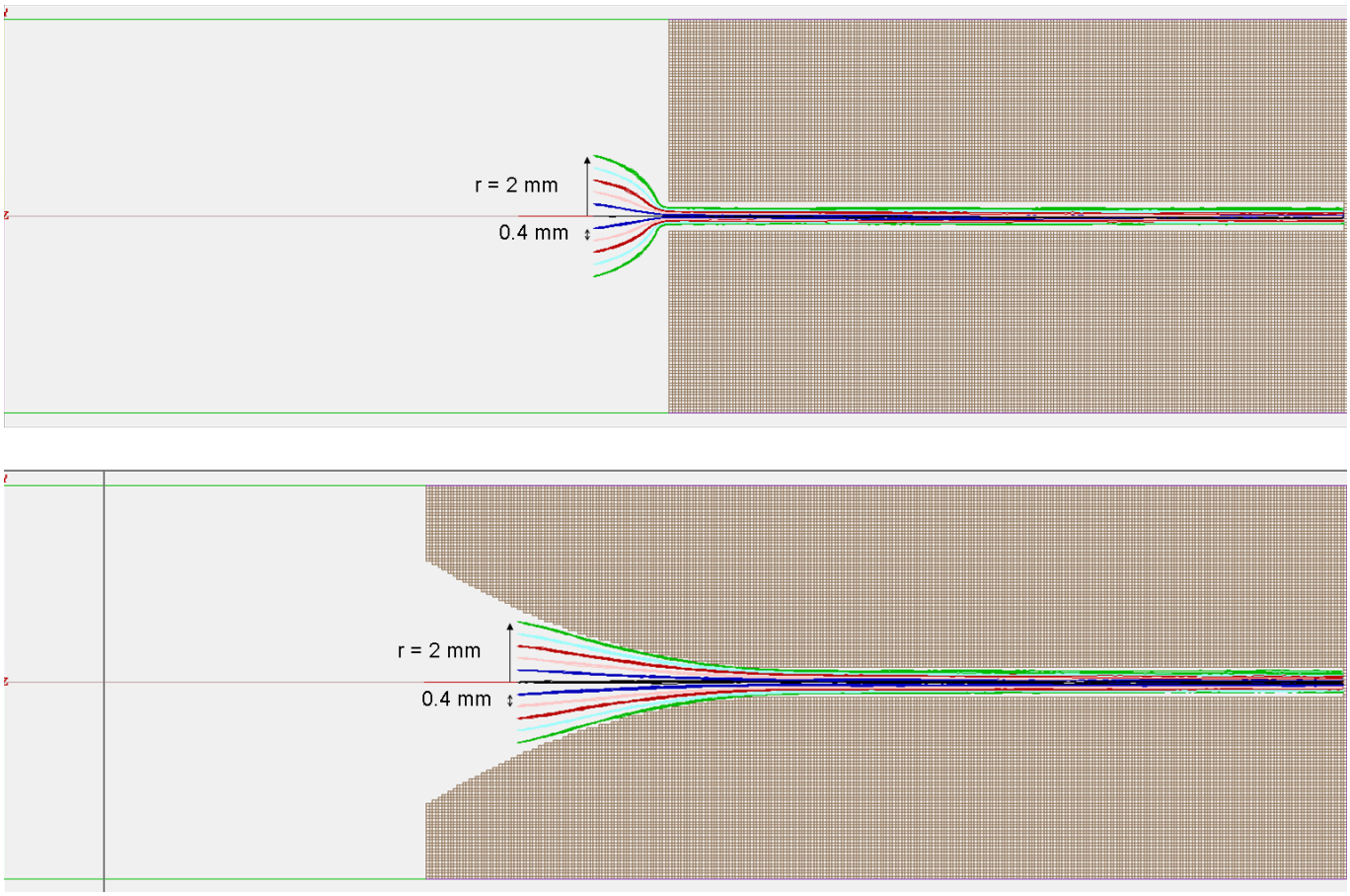

Figure S-6: trajectories of 10 ions starting 2.5 mm beyond the ion emitter at various radial positions between r = 0 mm and r = 2 mm.

S-V/ Ultrahigh Vacuum Deposition of CytC

CytC (Aldrich D7752) was dissolved in a water/methanol mixture to which 2% formic acid (Fluka 94318) was later added. The same ion source as the one described previously has been used for the gas phase ion generation, apart that the capillary diameter is 0.5 mm in this case. The ions in vacuum are guided through six differentially pumped stages to reach a pressure below 10^{-10} mbar at the sample position.[4, 5] The first vacuum chamber is equipped with a rf-ion funnel. A rf-quadrupole ion guide in the second pumping stage is used to select the required m/z-section of the protein ion beam, which is monitored by the time-of-flight mass spectrometer downstream. On the substrate position in UHV, mass selected ion currents of 100–1500 pA were detected and decelerated to a kinetic energy of 2–5 eV per charge before deposition. The coverage is monitored via a current measurement at the sample position using electrometers (Keithley 617).

A Cu(111) surface has been used for deposition. This surface was prepared in an integrated UHV preparation setup at a base pressure of 3×10^{-10} mbar. The metal crystal was repeatedly sputtered by argon ions and annealed. The sample is then transferred in situ to the deposition chamber and subsequently to the STM without breaking the ultrahigh vacuum.

S-VI/ Mass Spectrometry

High resolution mass spectra of a positive ion mode calibration mix (Thermo Fisher Scientific, Dreieich, Germany) containing caffeine (20 µg/ml), MRFA (1 µg/ml) and Ultramark 1621 (0.001%) in an acetonitrile (50%), methanol (25%) and acetic acid (1%) aqueous solution have been recorded on an Orbitrap XL ETD mass spectrometer (Thermo Fisher Scientific, Bremen, Germany). The solution was delivered at a constant flow rate of 500 nl/min using the built-in syringe pump. The mass spectrometer was equipped with a nano-electrospray ion source (Proxeon Biosystems, Odense, Denmark) and the electrospray voltage of 2.5 kV was applied via a liquid junction.

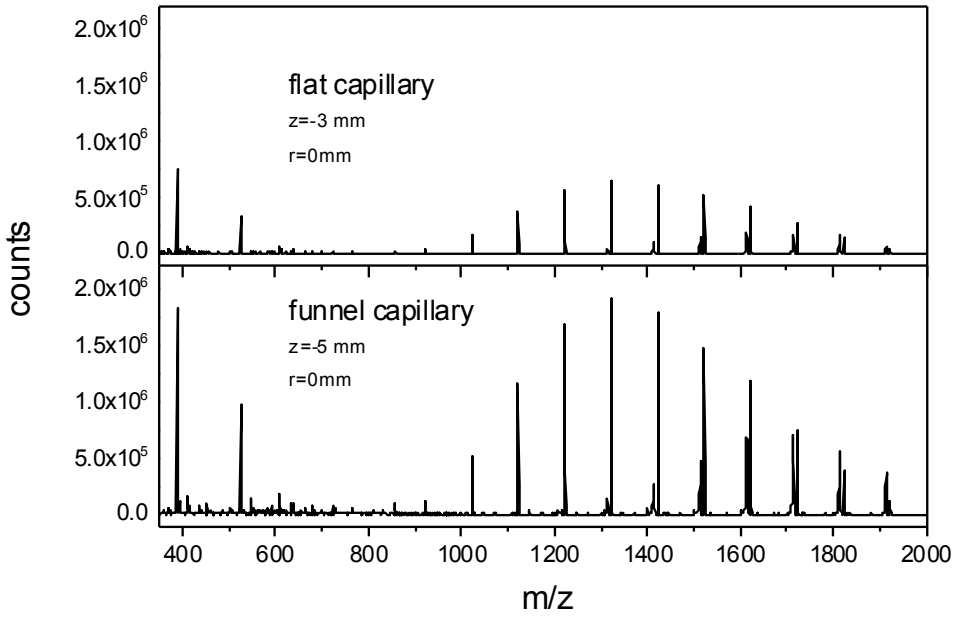

Figure S-7: High resolution mass spectra of the positive ion mode calibration solution recorded with an Orbitrap XL ETD mass spectrometer for the flat and the funnel capillaries.

These mass spectra have been recorded with a 0.5 mm diameter funnel shaped capillary. The small diameter (comparable to the commercial capillaries usually used) ensures that the vacuum is maintained without any modification of the pumping equipment. As a consequence the effect of the funnel inlet on the enhancement of the transmission is small in comparison to the 1 mm or 0.75 mm diameter capillaries. The improvement in intensity measured by the mass spectrometer is comparable to the signal increase known to flared capillary inlets.[7] This agrees with our model, which requires a high velocity gas flow in the funnel to collimate the ions. Since we use the same funnel cross section (i.e. the funnel has the same 8 mm diameter opening for both capillaries although the diameter of the cylindrical part of the capillary is different), the velocity in the funnel is at least reduced by a factor of 4 when going from 1 mm to 0.5 mm in capillary diameter. Furthermore, the capillary used here is much longer (15 cm compared to 6 cm), which induces higher losses in the capillary itself.

Nevertheless, the mass spectra obtained with the standard and with the modified capillaries are equivalent with no additional background peaks, which show that we have no disturbing influences from the funnel inlet either.

S-VII/ Temperature Dependence

All data reported in the manuscript was measured for an interface temperature of 180°C. The temperature of the interface is the crucial parameter for the complete desolvation of the droplets. If the temperature is too low, large clusters or even droplets can be generated.

We therefore measured the currents in the ion source as function of temperature for 10^{-4}M Rho solution at 2.5 kV spray voltage with the emitter within the funnel at z=-6.5mm. While the emission stays constant, we found a significant transition in the transmittance around 125°C, jumping from 20% to 75%, reaching the space charge limit of that particular emitter, which was 30nA. Around the same temperature the sound of droplet impact on the hot capillary surface disappears and the detected currents become more stable. We interpret this behavior as the transition from a cloud of droplets to a properly desolvated ion cloud.

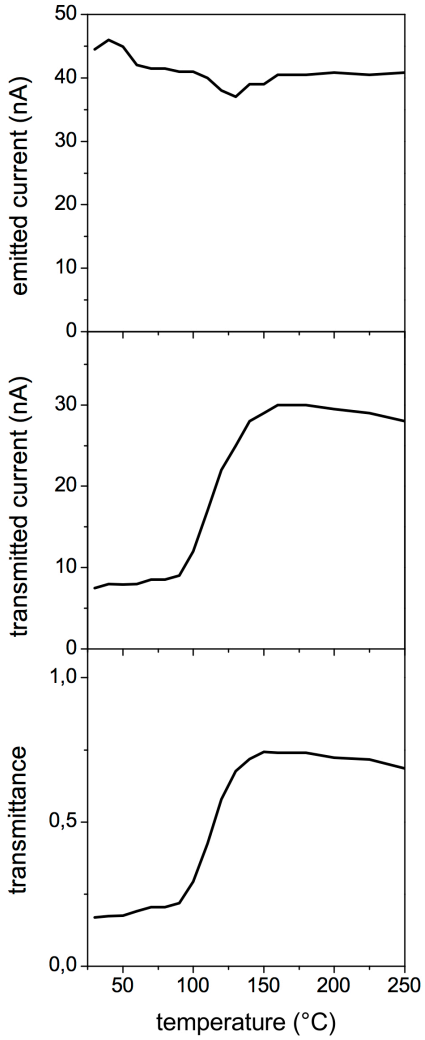

Figure S-8: Temperature dependence of the transmission of the funnel interface of a 1mm capillary. V_{ES}=2.5kV, RhoB c=10^{-4} M, z=-6.5mm.

S-VIII/ Sampling Efficiency

Following Schneider et al.[8] sampling efficiency is defined as the ratio of molecular ions detected in vacuum and molecules entering the source in solution. We can estimate the sampling efficiency based on the flow rate (f = 500 nL/min) and analyte concentration (c = 10^{-5} M and 10^{-4} M) as well as on the transmitted current (approx. 10 nA and 40 nA for both concentrations respectively for the 1 mm diameter capillary), assuming that the ion current detected relates to analyte ions, what is shown in the section 'chemical characterization'. The maximal emission currents for the case that all analyte molecules from solution are ionized is

$$I_{max}(c) = c\, f\, N_A\, q\,.$$

For singly charged ions we find for the above numbers $I_{max}(10^{-5}\ M) = 8$ nA and $I_{max}(10^{-4}\ M) = 80$ nA. We see in the experiements, for instance in Figures 2 and 3 or in Figure S8, that up to 10 nA are transferred without losses for 10^{-5} M, and up to 40 nA for 10^{-4}M. Thus for 10^{-5}M the ion source provides close to 100% ionization efficiency and hence a similar sampling efficieny as we detect all of the emitted current. At 10^{-4}M the transmittance may still be 100%, however only when not all ions get ionized. As we find only 40 nA maximal transmittance, we seem to be limited to a sampling efficiency of 50%, however this is due to ionization efficieny rather that ion transmission. If more ions are generated by increasing voltage and concentration further, the efficiency becomes lower because the space charge limit of 40 nA remains, while the current rises. This is consistent with the finding of Schneider et al. who also observe a reduced sampling efficiency when increasing the concentration, however in their case from 10^{-9} M to 10^{-8} M.[8]

S-IX/ Reproducibility

In the course of this study, numerous experiments with many different capillaries were conducted. In Figure S8 the transmitted current as a function of emitted current for an emitter position of z = -6.5 mm, r = 0 mm at a concentration of 10^{-4} M is shown for several experiments with a 1 mm funnel capillary. These curves are obtained by plotting the $I_{emitted}(V_{spray})$ vs. the $I_{transmitted}(V_{spray})$ parameterized by the spray voltage V_{spray}. In this plot the diagonal corresponds to 100% transmission, which is reached for all data sets up to a maximum current above which the transmittance drops. The value of this threshold current is different for the various emitters used. Further, we compare the data for the 1 mm funnel capillary to that for the same funnel inlet attached to 0.75 mm and 0.5 mm capillaries. We see that the 0.75 mm capillary shows the same behaviour, but does not reach 40 nA of maximal current.

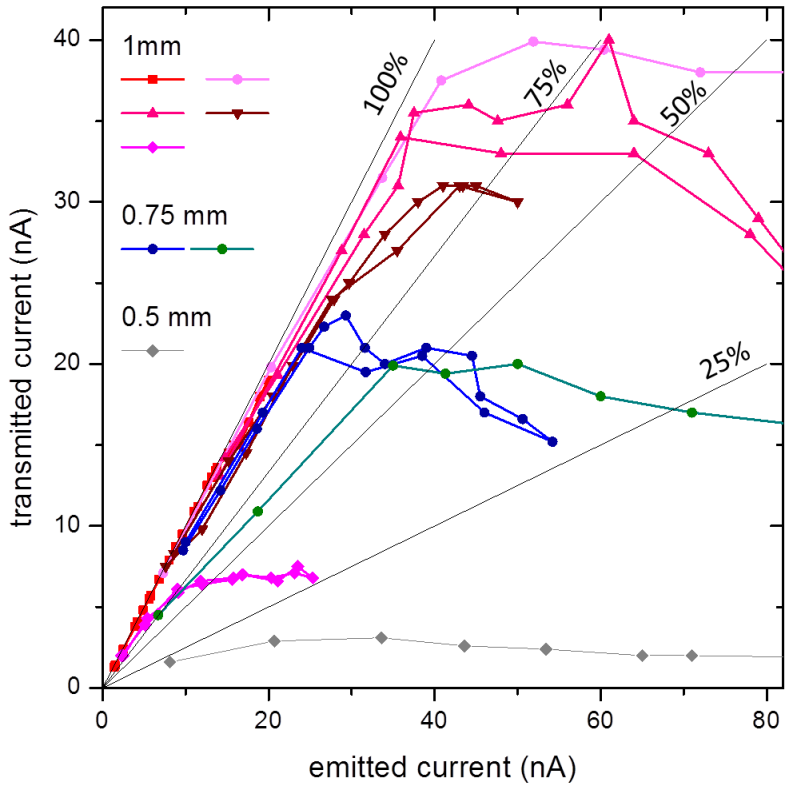

Figure S-9: Transmitted current as a function of emitted current at V_{ES} = 2.5 kV for the 1 mm funnel capillary . The emitter was placed at z = -6.5mm, r = 0mm and fed with the 10^{-4}M RhoB solution. For comparison, corresponding data are given for the same funnel inlet attached to 0.75 mm and 0.5 mm capillaries.

References

1. Sesterhenn, J., A characteristic-type formulation of the Navier–Stokes equations for high order upwind schemes. *Comput. Fluids* 2000, 30, 37-67.

2. Dahl, D. A., Simion for the personal computer in reflection. *Int. J. Mass spectrom.* 2000, 200, 3-25.

3. Appelhans, A. D.; Dahl, D. A., SIMION ion optics simulations at atmospheric pressure. *Int. J. Mass spectrom.* 2005, 244, 1-14.

4. Rauschenbach, S.; Stadler, F. L.; Lunedei, E.; Malinowski, N.; Koltsov, S.; Costantini, G.; Kern, K., Electrospray Ion Beam Deposition of Clusters and Biomolecules. *Small* 2006, 2, 540-547.

5. Deng, Z.; Thontasen, N.; Malinowski, N.; Rinke, G.; Harnau, L.; Rauschenbach, S.; Kern, K., A Close Look at Proteins: Submolecular Resolution of Two- and Three-Dimensionally Folded Cytochrome c at Surfaces. *Nano Lett.* 2012, 12, 2452-2458.

6. Wu, S.; Zhang, K.; Kaiser, N. K.; Bruce, J. E.; Prior, D. C.; Anderson, G. A., Incorporation of a Flared Inlet Capillary Tube on a Fourier Transform Ion Cyclotron Resonance Mass Spectrometer. *J. Am. Soc. Mass. Spectrom.* 2006, 17, 772-779.